Available online at www.sciencedirect.com

SCIENCE DIRECT

Free Radical Biology & Medicine 38 (2005) 557–567

www.elsevier.com/locate/freeradbiomed

Original Contribution

Redox properties of the lipocalin α_1-microglobulin: Reduction of cytochrome *c*, hemoglobin, and free iron

Maria Allhorn[a], Anna Klapyta[b], Bo Åkerström[a,*]

[a]*Department of Cell and Molecular Biology, Lund University, BMC, B14, 221 84 Lund, Sweden*
[b]*Department of Physical Biochemistry, Jagiellonian University, Krakow, Poland*

Received 13 July 2004; revised 26 October 2004; accepted 1 December 2004
Available online 21 December 2004

Abstract

α_1-Microglobulin (α_1m) is a 26-kDa plasma and tissue glycoprotein. The protein has a heterogeneous yellow-brown chromophore consisting of small unidentified prosthetic groups localized to a free thiol group (C34) and three lysyl residues (K92, K118, and K130) around the entrance to a hydrophobic pocket. It was recently reported that α_1m can bind heme and that a C-terminally processed form of α_1m degrades heme. It is shown here that α_1m has catalytic reductase and NADH-dehydrogenase-like activities. Cytochrome *c*, nitroblue tetrazolium (NBT), methemoglobin, and ferricyanide were reduced by α_1m. Comparison of the reduction rates suggests that methemoglobin is a better substrate than cytochrome *c*, NBT, and ferricyanide. The reactions with cytochrome *c* and NBT were mediated by superoxide anions since they were inhibited by superoxide dismutase. The addition of the biological electron donors NADH, NADPH, or ascorbate enhanced the reduction rate of cytochrome *c* approximately 30-fold. Recombinant α_1m, which has much less chromophore than plasma and urine α_1m, was a stronger reductant than the latter α_1m forms. Site-directed mutagenesis of C34, K92, K118, and K130 and thiol group chemistry showed that the C34 thiol group was involved in the redox reaction but relies upon cooperation with the lysyl residues. The redox properties of α_1m may provide a physiological protection mechanism against extracellularly exposed heme groups and other oxidants.

Keywords: α_1-Microglobulin; Reductase; Electron; Superoxide anions; Heme; Hemoglobin; Iron; NAD(P)H; Dehydrogenase

Introduction

The Lipocalins is a protein superfamily with 30–35 members distributed among animals, plants, and bacteria [1,2]. The members of the superfamily have a highly conserved three-dimensional structure but very diverse functions. The lipocalin fold consists of eight antiparallel β-strands folded into a barrel with one closed and one open end. The interior of the barrel forms a binding site for small hydrophobic ligands and this structural property is the basis for a surprisingly wide array of biological functions. Retinol-binding protein and prostaglandin D synthase from mammals, insect bilin-binding protein, and plant violaxanthin-de-epoxygenase are examples of lipocalins [3–6].

α_1-Microglobulin (α_1m) is one of the originally described lipocalins [7,8] and perhaps also the most widespread member phylogenetically [9,10]. So far, it has been found in mammals, birds, fishes, and amphibians. α_1m has a number of intriguing and unusual properties. For example, it has a yellow-brown color and is charge heterogeneous. This is caused by an array of small chromophore prosthetic groups

Abbreviations: α_1m, α_1-microglobulin; C34S-α_1m, α_1-microglobulin mutated at amino acid position 34; K(3)T-α_1m, α_1-microglobulin mutated at amino acid positions 92, 118, and 130; t-α_1m, truncated α_1-microglobulin without C-terminal tetrapeptide LIPR; EDTA, ethylenediamineteraacetic acid; [^{14}C]IAA, iodo-[^{14}C]acetamide; LIPR, leucine-isoleucine-proline-arginin; NADH, nicotinamide adenine dinucleotide; NAD^+, oxidized NADH; NADPH, nicotinamide adenine dinucleotide phosphate; NBT, nitroblue tetrazolium; NEM, *N*-ethylmaleimide; PBS, phosphate buffer saline; r_i, initial reaction rate; ROS, reactive oxygen species; SDS-PAGE, sodium dodecyl sulfate-polyacrylamide gel electrophoresis; SE, standard error; SOD, superoxide dismutase.

* Corresponding author. Fax: +46 46 157756.
E-mail address: bo.akerstrom@medkem.lu.se (B. Åkerström).

0891-5849/$ - see front matter © 2004 Elsevier Inc. All rights reserved.
doi:10.1016/j.freeradbiomed.2004.12.013

attached to the amino acid residues C34, K92, K118, and K130, which are localized around the entrance of the lipocalin pocket [11,12]. α_1m is found in blood and in connective tissue in most organs and is most abundant at interfaces between the cells of the body and the environment, such as in lungs, intestine, kidneys, and placenta [13–16]. α_1m has immunosuppressive properties, such as inhibition of antigen-induced proliferation of human peripheral lymphocytes, migration and chemotaxis of granulocytes [17,18], IL-2 production by T-cells [19], and activation of the mononuclear cells [20].

Recently, it was shown that α_1m can bind heme/hemin strongly and that a processed form of α_1m (t-α_1m) which is formed by cleavage of the C-terminal tetrapeptide LIPR during incubation with erythrocyte membranes or purified hemoglobin has heme-degrading properties [21]. In chronic leg ulcers, a hemolytic inflammatory condition where free heme and iron are considered to be pathogenic factors, α_1m was found to bind to heme and colocalized with heme, and t-α_1m was continuously formed [22]. This suggests that α_1m has a role in heme catabolism and may be part of the extracellular protection mechanisms against the deleterious oxidative effects of exposed heme proteins and heme groups. Another abundant heme protein is cytochrome *c*, a mitochondrial electron transporter of the respiratory chain. Due to its water-soluble properties, cytochrome *c* may be exposed to surrounding tissue components during, for instance, inflammation and other necrotic conditions, and is a potential oxidative threat via its heme group. Therefore, we investigated the interactions between α_1m and cytochrome *c*.

Heme, which is linked covalently to cytochrome *c*, consists of the organic compound protoporphyrin IX chelate binding an iron atom. The iron atom acts as an electron acceptor or donor by oscillating between the Fe^{2+} (ferrous) and Fe^{3+} (ferric) oxidation levels. In a neutral buffer, cytochrome *c* is mainly found in the oxidized Fe^{3+} form. Here, we show that α_1m reduces cytochrome *c* to the Fe^{2+} form, via formation of superoxide anion radicals ($O_2^{\bullet -}$) and using the biological electron donors ascorbate and NADH/NADPH as cofactors. The protein also reduces methemoglobin and free ferric iron, as well as the synthetic electron acceptor nitroblue tetrazolium (NBT). We have investigated the details of this reductase-like property and speculate that it may be part of a heme-degradation mechanism and may constitute a novel antioxidation defense system.

Materials and methods

Recombinant α_1m

Wild-type and mutated variants of α_1m were expressed in *Escherichia coli* (*E. coli*). Using site-directed mutagenesis a Cys → Ser substitution was introduced at amino acid position 34 in the C34S-α_1m mutant, and Lys → Thr substitutions at positions 92, 118, and 130 in the K(3)T-α_1m mutant. In the recombinant α_1m forms, the N-terminus was elongated by an amino acid sequence containing eight histidines (His-tag) and an enterokinase cleavage site (DDDDKA). The purity of all recombinant α_1m variants was estimated by SDS-PAGE. The results showed distinct protein bands identified as α_1m by Western blotting and N-terminal sequencing. A correct folding of the proteins was confirmed using far-UV-circular dichroism spectroscopy (Klapyta et al., manuscript in preparation). The His-tag was removed by incubating 10 mg α_1m with 400 U enterokinase (Sigma Aldrich Sweden AB) for 5 h at room temperature in 20 mM Tris-HCl, 0.5 M NaCl, pH 8.0. His-tag-free α_1m was then separated from enterokinase by gel chromatography and the N-terminal amino acid sequence determined.

Proteins and reagents

Human α_1m was prepared from plasma [23], urine [24], and baculovirus-infected insect cells [25] as described. T-α_1m was prepared from plasma or recombinant α_1m by incubation with ruptured erythrocytes as described [21]. Mouse monoclonal anti-α_1m, BN11.10, was prepared and purified as described [26] and immobilized to Affi-Gel Hz (Bio-Rad Labs, Hercules, CA) at 20 mg/ml following instructions from the merchant. All other proteins were of analytical grade and were purchased from Sigma Chemicals, St Louis, MO, if not indicated otherwise. Nitroblue tetrazolium was from Boehringer Mannheim GmbH, Mannheim, Germany. Reagent solutions were prepared using Millipore-filtrated water. A His_8-tag peptide was synthesized at Chemical Research and Development Laboratory, KJ Ross-Petersen ApS, Holte, Denmark. The purity of the peptide was analyzed by HPLC and was estimated to be >95%.

Reduction of cytochrome c

Bovine heart cytochrome *c* at the concentrations 6–50 μM was mixed with plasma α_1m, recombinant α_1m, or the control proteins ovalbumin and orosomucoid at 5–40 μM. The buffer used in these reactions was either PBS (10 mM sodium phosphate, pH 7.4, 120 mM NaCl, 3 mM KCl) or 20 mM Tris-HCl, pH 7.4, 150 mM NaCl. For pH studies 20 mM sodium phosphate, 100 mM NaCl at pH 6 and 7 or 20 mM Tris-HCl, 100 mM NaCl at pH 8 and 9, were used. The reduction of cytochrome *c* was measured as an increase of the absorbance at 550 nm as described below. Where indicated, the reactions were performed with the addition of 3 μM superoxide dismutase, 1 mM KCN. or 10 mM NaN_3. In one experiment α_1m was first preincubated with cytochrome *c* immobilized to CNBr-activated Sepharose 4B at 10 mg protein/ml gel (Amersham Pharmacia Biotech AB, Sweden) at the molar α_1m:cytochrome *c* ratio 1:15 or only Sepharose, for 5 h. After centrifugation at 1000 *g* for 5 min, the supernatants were analyzed for cytochrome *c*

reduction as described above. Freshly made solutions of *N*-ethylmaleimide (NEM), NADH, NADPH or ascorbic acid were added to the reaction mixtures at the final concentrations 2–250 μM as indicated.

NADH oxidation

NADH oxidation was followed by measuring the reduction of the absorbance at 340 nm in a mixture containing 10 μM α_1m, 10 μM cytochrome *c*, and 20 μM NADH in 20 mM Tris-HCl, pH 7.6. The molar concentration of NAD^+ was calculated using the extinction coefficient 6.3×10^3 (M^{-1} cm^{-1}).

Reduction of nitroblue tetrazolium

Measurements of NBT reduction were performed in 10 mM Tris-HCl, pH 8.5, using NBT at 200 μM, α_1m at final concentrations between 1.25 and 10 μM and/or NADH, NADPH, or ascorbate at final concentrations of 2–250 μM. In control experiments, KCN or NaN_3 was added to 1 or 10 mM final concentration, respectively. The reduction of NBT was measured as an increase of the absorbance at 530 nm as described below.

Methemoglobin reduction

Human methemoglobin, 2.5–50 μM, was incubated at room temperature with 40 μM α_1m or orosomucoid in 20 mM Tris-HCl, 100 mM NaCl, pH 7.4. Absorbance at 630 nm was recorded at 1-min intervals and absorbance spectra were recorded after 30 min.

Ferricyanide reduction

α_1m, 5–40 μM in 20 mM Tris-HCl, pH 7.4, 150 mM NaCl, was incubated with 500 μM potassium ferricyanide ($K_3Fe(CN)_6$) at room temperature for 90 min. The amounts of produced ferrocyanide were determined using bathophenanthrolinedisulfonic acid (Sigma Chemicals) as described by Avron and Shavitt [27] by measuring the increase of absorbance at 535 nm and using the reagents as a blank.

Spectrophotometric methods

Kinetic studies were made by recording absorbance values for 20 min with 1-min intervals on a Beckman DU 640i spectrophotometer. Absorbance spectra were measured using a scan rate of 1200 nm/min in the UV-VIS region between 250 and 700 nm. Initial reaction rates, r_i, were calculated from the Δ-absorbance after 5 or 10 min and using the extinction coefficients $2.1 \times 10^4 M^{-1}$ cm^{-1} for the cytochrome *c* $Fe^{3+/2+}$ transition, 1.5×10^4 M^{-1} cm^{-1} for the reduction of NBT, and $3.7 \times 10^3 M^{-1}$ cm^{-1} for the reduction of methemoglobin [28].

Electrophoresis

SDS-PAGE was performed using 12% gels in the buffer system described by Laemmli [29] including 2% vol/vol β-mercaptoethanol in the sample buffers. High-molecular-mass standards (Rainbow markers; Amersham Pharmacia Biotech, Uppsala, Sweden) were used.

Analysis of free thiol groups

α_1m was incubated with iodo-[^{14}C]acetamide ([^{14}C]IAA) (Amersham Life Science, specific activity 59.0 mCi (2.2 GBq)/mmol). The reaction mixtures contained 2 μM α_1m in 0.2 M Tris-HCl, pH 8.5, and 1 mM [^{14}C]IAA. The reaction proceeded for 60 min at 25°C in the dark. To determine the amounts of bound [^{14}C]IAA, the alkylated α_1m was subjected to SDS-PAGE and phosphoimaging.

Results

Reduction of cytochrome c

The heme group of *c*-type cytochromes contains iron, which can change from the oxidized (Fe^{3+}) to the reduced (Fe^{2+}) form. It was observed initially that plasma α_1m and recombinant α_1m ("α_1m") induced a reduction of cytochrome *c* to the Fe^{2+} form, shown spectrophotometrically in Fig. 1 as the appearance of two absorbance peaks at 520 and 550 nm. The reaction was completely inhibited by superoxide dismutase (SOD), indicating that superoxide anions are involved in the reduction. Recombinant α_1m is equipped with an N-terminal His_8-tag but removal of this (see Materials and methods) did not decrease the reducing effect, and a synthetic His_8-peptide alone did not reduce cyto-

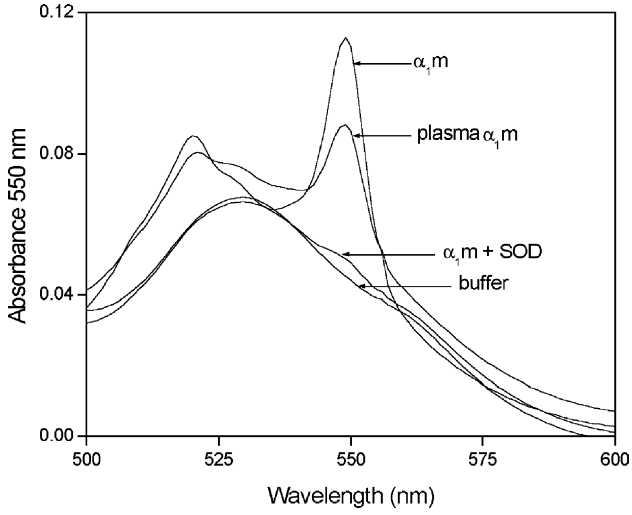

Fig. 1. Reduction of cytochrome *c* by α_1m. Absorbance spectra of 6 μM cytochrome *c* in PBS, incubated for 3 h with 10 μM α_1m (recombinant), 10 μM plasma α_1m, 10 μM α_1m + 3 μM SOD, or buffer. The reagents without cytochrome *c* were used as blanks.

chrome *c*. The reduction reaction was not inhibited by the addition of EDTA, suggesting that chelatable metal ions are not involved. No inhibition was seen when KCN or NaN_3 was added, suggesting a nonheme reaction of α_1m. The concentration of KCN used (1 mM) was shown to have no effect on cytochrome *c* [30].

The time dependence of the reduction reaction was followed by reading the absorbance at 550 nm of a 50 μM solution of cytochrome *c* and various concentrations of α_1m at regular intervals (Fig. 2A). The rate of the reaction increased with increasing α_1m concentrations and using 40 μM α_1m the rate was initially high but declined slowly, consistent with depletion of the substrate. No reaction was seen when 3 μM SOD was added to cytochrome *c* with 20 μM α_1m (Fig. 2A). The initial reaction rate, r_i, was plotted as a function of the concentration of α_1m (Fig. 2B). A faster reaction was observed with recombinant α_1m compared to plasma α_1m (Fig. 2B), urine α_1m, and recombinant α_1m expressed by insect cells (not shown). A sigmoidal concentration dependence was seen for α_1m, indicating that the protein acts as both a catalyst and a substrate in the reaction. Above 10 μM, the rate constant of the reaction was 1.2×10^{-4} (s^{-1}) for recombinant α_1m and 0.4×10^{-4} (s^{-1}) for plasma α_1m. Orosomucoid, another member of the lipocalin family, did not show any ability to reduce cytochrome *c* (Fig. 2B). The pH dependence of the reaction, measured at 10 min, is shown in Fig. 2C. A several-fold increased reaction rate was observed at pH 8 and 9 compared to pH 6 and 7.

Effect of α_1m variants

The influence of the C34 thiol group of α_1m for the reaction was studied. Fig. 3A shows that the C34S-α_1m mutant had only a weak reducing effect on cytochrome *c*, indicating that the thiol group is involved in the reaction. This was supported by blocking the thiol group with 300 μM *N*-ethylmaleimide, which resulted in an inhibition of the reduction (Fig. 3B). As a control, it was shown that the same concentration of *N*-ethylmaleimide had no inhibitory effect of the cytochrome *c* reduction by 20 μM vitamin C. Human albumin, which also has one free thiol group, did not reduce cytochrome *c* under these conditions (not shown).

Two other α_1m variants were studied. The K(3)T-α_1m mutant had a much weaker reducing activity than wild-type α_1m (Fig. 3A), showing that the three chromophore-carrying lysyl residues are essential for the reaction even though the C34 thiol group is present (see also below). Finally, t-α_1m, a naturally occurring form of α_1m with heme-degrading properties and lacking the C-terminal tetrapeptide LIPR, reduced cytochrome *c* much faster than wild-type α_1m, with r_i values of 2.0 and 0.32 nM/s, respectively (Fig. 3C).

Interaction with NADH, NADPH, and ascorbate

NADH strongly enhanced the reduction of cytochrome *c* by α_1m. Fig. 4A shows that 250 μM NADH increased the rate of reduction by 10 μM α_1m almost 30-fold (Table 1). A 250 μM NADH did not show any reducing activity on its own. These results indicate dehydrogenase properties of α_1m, i.e., an electron transfer from NADH to α_1m. Fig. 4B shows that the reduction in the presence of NADH was inhibited by SOD, indicating superoxide anions as mediators of the reduction also when NADH is present. A weak remaining activity, however, suggests that a minor superoxide-independent reduction mechanism also may be involved. The C34S- and K(3)T-α_1m mutants displayed a slower reduction of cytochrome *c* than wild-type α_1m in the presence of NADH (Fig. 4C). 1. A stronger accelerating effect of NADH was obtained with K(3)T-α_1m as compared to C34S-α_1m (Table 1), suggesting that the C34 thiol, but not K92, K118, and K130 are critical for the interaction with NADH. 1Interestingly, only weak increases of the reaction

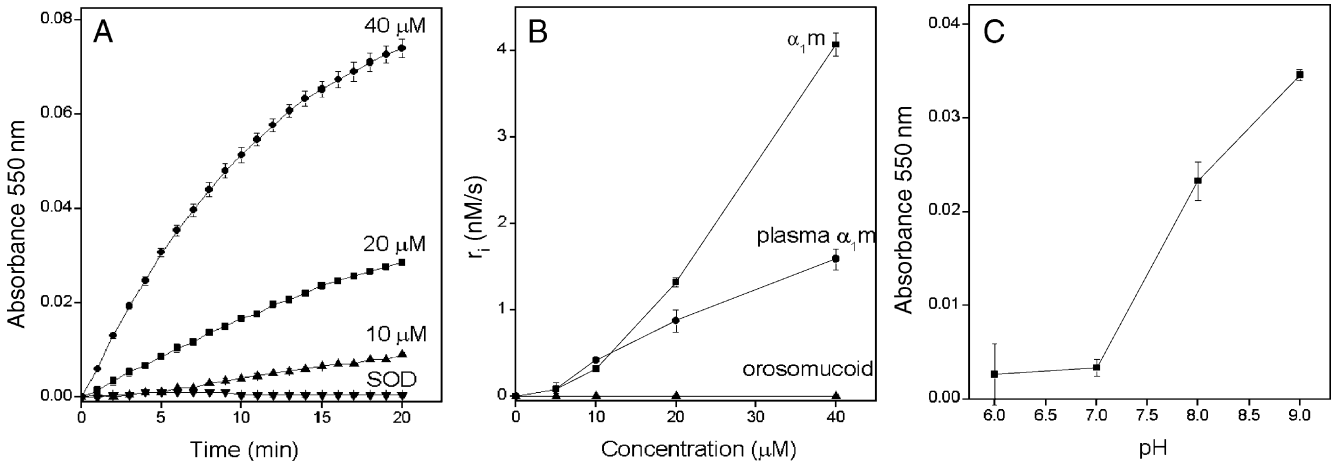

Fig. 2. Characterization of the reduction of cytochrome c by α_1m. (A) Time dependence. The absorbance at 550 nm of 50 μM cytochrome *c* and various concentrations of α_1m, or 50 μM cytochrome *c*, 20 μM α_1m, and 3 μM SOD was read at 1-min intervals. (B) Concentration dependence. The initial reaction rates (r_i) were calculated from the net absorbance increase after 10 min of 50 μM cytochrome *c* plus various concentrations of α_1m, plasma α_1m, and orosomucoid, and plotted as a function of the α_1m concentration. (C) pH dependence. The net absorbance increase at 550 nm of mixture of cytochrome *c* (50 μM) and α_1m (40 μM) was read after 5 min at pH 6, 7, 8, and 9. Each point shows the mean of triplicates and SE.

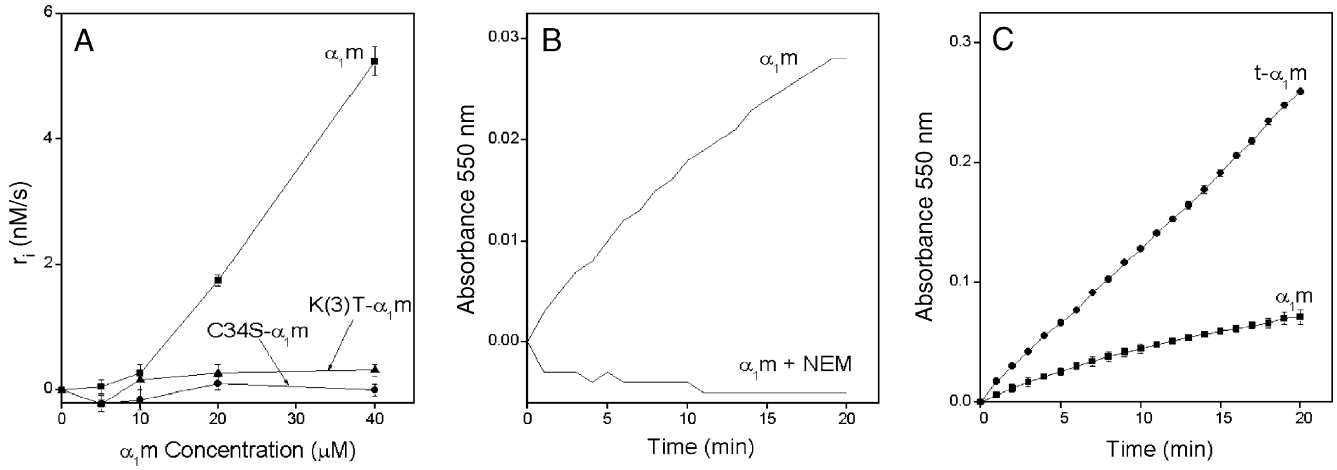

Fig. 3. Reduction of cytochrome *c* by different α_1m-forms. (A) The initial rates (r_i) were calculated from the net absorbance increase at 550 nm after 5 min for 50 μM cytochrome *c* plus various concentrations of α_1m, C34S-α_1m , or K(3)T-α_1m, and plotted as a function of the α_1m concentration. Each point shows the mean of triplicates and SE. (B) The absorbance at 550 nm of 50 μM cytochrome *c* and 20 μM α_1m, with or without 300 μM *N*-ethylmaleimide, was read at 1-min intervals. (C) The absorbance at 550 nm of 50 μM cytochrome *c* and 20 μM α_1m or 20 μM t-α_1m was read at 1-min intervals. Each point shows the mean of triplicates and SE.

rate was seen for t-α_1m in the presence of NADH, suggesting that the tetrapeptide LIPR is essential for the interaction with NADH. Fig. 4D shows a rapid initial formation of NAD^+, the oxidized equivalent of NADH, during the NADH-assisted reduction of cytochrome *c* by α_1m. The NAD^+ production declined, however, after 1 min, suggesting that other reaction

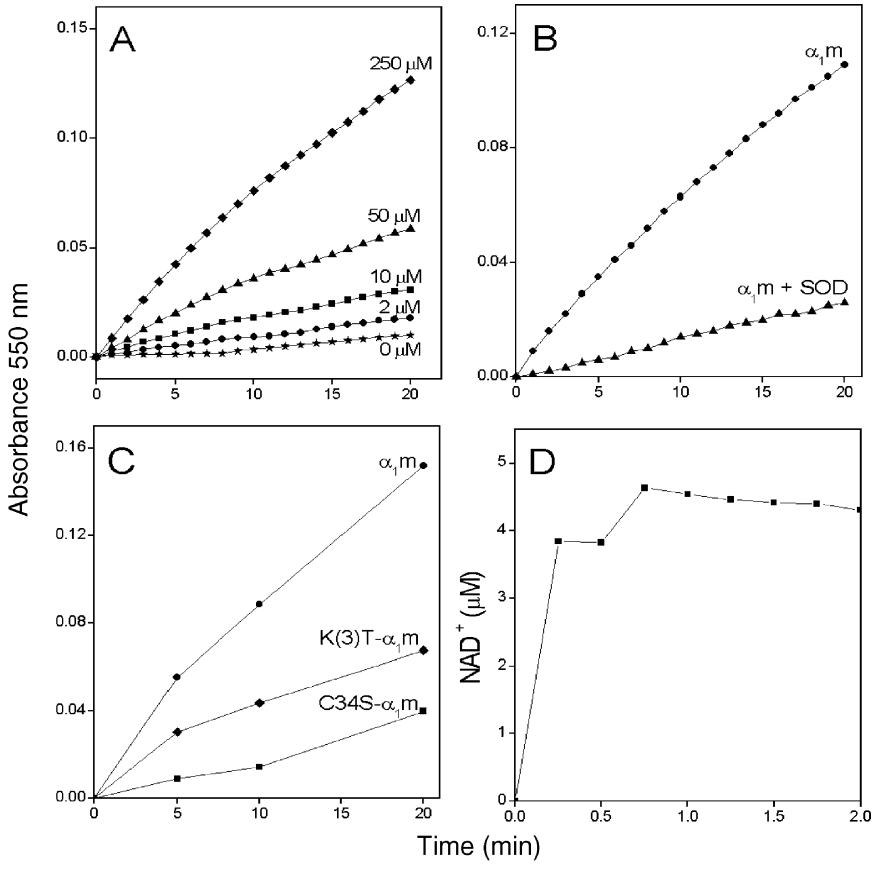

Fig. 4. Acceleration of cytochrome *c* reduction with NADH. (A) The absorbance at 550 nm of 20 μM cytochrome *c*, 10 μM α_1m, and NADH at various concentrations was read at 1-min intervals. (B) The absorbance at 550 nm of 50 μM cytochrome *c*, 10 μM α_1m, and 50 μM NADH, with or without 1.5 μM SOD, was read at 1-min intervals. (C) The absorbance at 550 nm of 50 μM cytochrome *c*, 10 μM α_1m, C34S-α_1m, or K(3)T-α_1m and 50 μM NADH was read at 5-min intervals. (D) NAD^+ was measured in a mixture of 10 μM α_1m, 10 μM cytochrome *c*, and 20 μM NADH by reading the absorbance at 340 nm at 15-s intervals.

Table 1
Initial reaction rates of the reduction of cytochrome *c*, NBT, and methemoglobin by various forms of α_1m with or without NADH, NADPH, or ascorbate

	r_i[a] (nM/s)			
	–	NADH	NADPH	Ascorbate
Cytochrome *c*				
α_1m	0.32 (1.8)[b]	9.0	8.0	12.0
C34S-α_1m	0.21 (0.10)[b]	1.0	<0.05	<0.05
K(3)T-α_1m	0.16 (0.26)[b]	5.0	<0.05	11.7
NBT				
α_1m	5.0	3.0	4.0	7.0
C34S-α_1m	0.4	<0.05	<0.05	0.2
K(3)T-α_1m	4.0	0.3	2.0	23.0
Methemoglobin[c]				
α_1m	24			
C34S-α_1m	15			
K(3)T-α_1m	21			

[a] Cytochrome *c* (50 μM), NBT (200 μM), methemoglobin (50 μM) and α_1m (10 μM) were mixed with buffer (–) or NADH (50 μM), NADPH (50 μM), or ascorbate (50 μM). The initial reaction rates were calculated from the net absorbance increase at 550 nm after 5 min for cytochrome *c*, 530 nm for NBT, and the net decrease at 630 nm for methemoglobin.
[b] The rate of the reduction of cytochrome *c* without NADH, NADPH, or ascorbate was also measured using 20 μM α_1m.
[c] The effects of NADH, NADPH, and ascorbate on the reactions with methemoglobin are not included because the high background activities of NADH, NADPH, and ascorbate prevented interpretation of the data.

products become more important at a later stage of the reaction.

Two other biological reductants, NADPH and ascorbate, also strongly accelerated the rate of reduction of cytochrome *c* by α_1m (Fig. 5), indicating that there was no preference for NADH as a reducing cofactor for α_1m. As expected, 50 μM ascorbate alone reacted rapidly with cytochrome *c* but a synergistic increase of the reaction rate by several factors was observed when when 20 μM α_1m was added (Fig. 5B). Table 1 summarizes the r_i values for the reactions with and without the reducing cofactors. In general, ascorbate was a better cofactor than NADH and NADPH, and the C34S-α_1m mutant interacted poorly with all cofactors.

Oxidation of α_1m

To test whether the reduction potential of α_1m was depleted during the reaction with cytochrome *c*, the protein was exposed for 3 h to a 15 molar excess of cytochrome *c*-Sepharose or free Sepharose as a control. After centrifugation, the supernatants containing α_1m were analyzed in a new incubation with cytochrome *c*. As shown in Fig. 6, the reaction rate of α_1m incubated with cytochrome *c*-Sepharose decreased markedly, indicating a depletion, i.e., oxidation of α_1m. The reaction rate increased again after addition of NADH, suggesting a regeneration of the reduced form.

The size, charge, and redox status of the free thiol group of α_1m during the reactions with cytochrome *c* and NADH were investigated. No detectable shifts of the mobility of α_1m on SDS-PAGE or nonreducing PAGE were observed (Figs. 7A and B). However, an oxidation of the free thiol group by cytochrome *c* is indicated by the decreased incorporation of [^{14}C]IAA in the presence of cytochrome *c* (Fig. 7C, wt, lanes 1 and 2). As expected, no labeling of the C34S-α_1m mutant was observed. Interestingly, the thiol group of K(3)T-α_1m was not oxidized by cytochrome *c* (Fig. 7C, K(3)T, lanes 1 and 2), indicating cooperativity between the C34 thiol group and the K92, K118, and K130 side chains in the reaction with cytochrome *c*. Finally, a stronger labeling by [^{14}C]IAA in the presence of NADH, i.e., a net reduction of the thiol group, was seen for both wt-α_1m and K(3)T-α_1m (Fig. 7C, lanes 3 and 4), explaining the increased reduction potential in the presence of NADH.

Reduction of NBT, methemoglobin, and free iron

The generation of superoxide anions by α_1m was confirmed by the reduction of NBT. An elevated absorbance

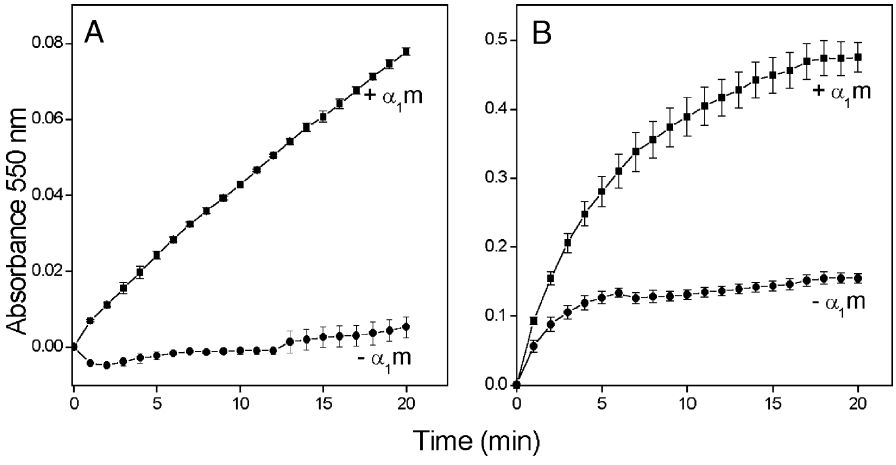

Fig. 5. Acceleration of cytochrome *c* reduction with NADPH and ascorbate. (A) The absorbance at 550 nm of 50 μM cytochrome *c* and 50 μM NADPH alone ("-α_1m") or with the addition of 5 μM α_1m ("+α_1m"), was read at 1-min intervals. (B) The absorbance at 550 nm of 50 μM cytochrome *c* and 50 μM ascorbate alone ("-α_1m") or with the addition of 20 μM α_1m ("+α_1m"), was read at 1-min intervals. Each point shows the mean of triplicates and SE.

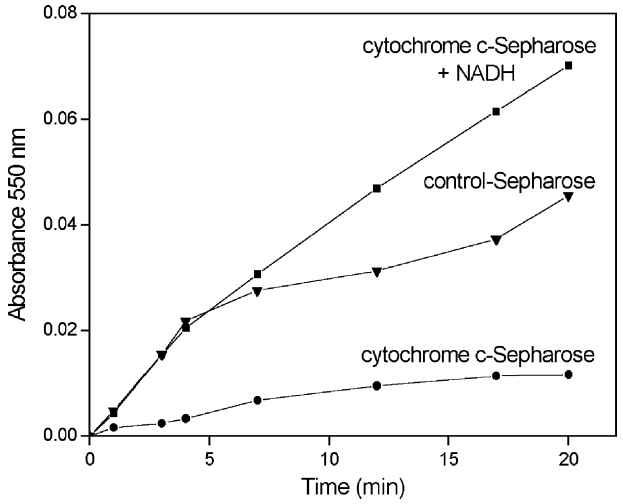

Fig. 6. Depletion of reducing potential of α_1m. α_1m (80 μM) was preincubated with 1.2 mM cytochrome *c*-Sepharose for 5 h and centrifuged. The supernatant was then diluted to the final α_1m concentration of 40 μM and incubated with 50 μM soluble cytochrome *c* (●) or cytochrome *c* and 250 μM NADH (■). As a control, α_1m was preincubated with unconjugated Sepharose for 5 h, centrifuged, and then incubated with soluble cytochrome *c* (▼). The absorbance at 550 nm of the solutions was read at different time points.

at 530 nm, a wavelength specific for reduced NBT, indicated reduction of NBT by recombinant α_1m (Fig. 8). The reaction accelerated in a dose-dependent way, a control protein (ovalbumin) was negative (Fig. 8A), and the reaction was inhibited to 80% by SOD (Fig. 8B). Similar to the reduction of cytochrome *c*, much less activity was seen with the mutant forms C34S-α_1m and K(3)T-α_1m (Fig. 8C), again indicating that the C34, K92, K118, and K130 side groups are involved in the reaction. The reaction rate was faster with NBT as a substrate ($k = 9 \times 10^{-4}$ s^{-1}) compared to cytochrome *c* ($k = 1.2 \times 10^{-4}$ s^{-1}). No inhibition of the reaction rates was seen when 1 mM KCN or 10 mM NaN_3 was added, suggesting a nonheme reaction for α_1m.

The oxidized variant of hemoglobin, methemoglobin, was rapidly reduced by α_1m. This was observed as a red-shift of the Soret band (Fig. 9A), an increase of absorbance peaks at 560 and 577 nm, and a decrease of the peak at 630 nm (Fig. 9B). The absorbance at 630 nm was plotted as a function of time (Fig. 9C), revealing a similar time frame for this reaction as above. SOD could not inhibit the methemoglobin reduction (Fig. 9C), indicating that superoxide anions were not involved in this case. The addition of NADH did not change the reaction rate (not shown).

Ferric cyanide (Fe^{3+}) is a strong artificial electron acceptor. Fig. 10 shows that α_1m has a concentration-dependent reducing effect on ferric cyanide to phenantroline-chelatable ferrous cyanide (Fe^{2+}) which has a specific absorbance peak at 535 nm. The reduction of ferricyanide by α_1m was not inhibited by SOD, and the addition of NADH did not accelerate the reaction rate (not shown).

The reduction of NBT was also studied in the presence of NADH, NADPH, and ascorbate and the initial reaction rates were measured (Table 1). The reduction of NBT by α_1m was accelerated marginally by ascorbate but not by NADH or NADPH. C34S-α_1m did not reduce NBT even in the presence of the cofactors but K(3)T-α_1m obtained an increased activity by the addition of ascorbate. These results thus support the data obtained with cytochrome *c*, i.e., that the C34 thiol but not K92, K118, and K130 is critical for the interaction with the cofactors. NADH, NADPH, and ascorbate alone reacted strongly with ferricyanide and methemoglobin, preventing interpretation of the results. Taken together, the data in Table 1 suggest that methemoglobin is a better substrate for the α_1m-reductase activity and ascorbate the preferred electron-donating cofactor.

Discussion

The present report shows that the plasma and tissue protein α_1m has cytochrome *c*, methemoglobin, and ferri-

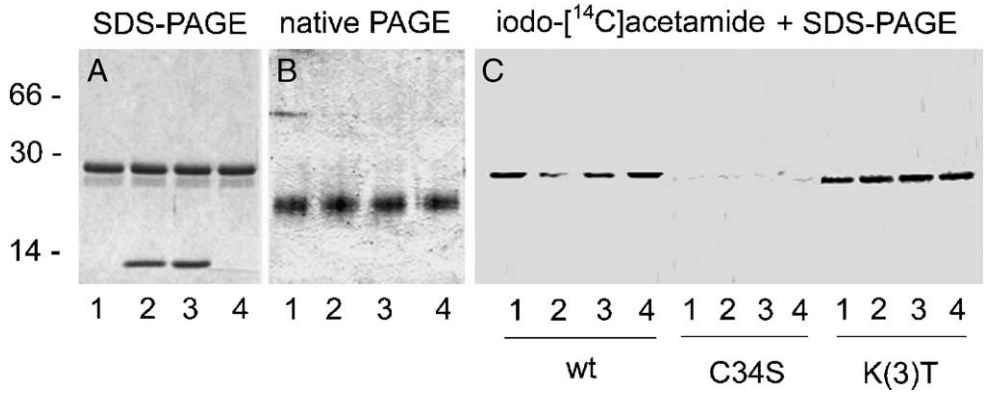

Fig. 7. Electrophoresis and thiol group labeling of α_1m. (A) SDS-PAGE with 2-mercaptoethanol or (B) nondenaturing PAGE of α_1m (lane 1), α_1m + cytochrome *c* (lane 2), α_1m, cytochrome *c* + NADH (lane 3), or α_1m + NADH (lane 4). Ten microliters of the samples was applied and the concentrations were 10 μM (α_1m), 10 μM (cytochrome *c*), and 50 μM (NADH). The gels were stained with Coomassie Brilliant Blue. (C) SDS-PAGE with 2-mercaptoethanol of 10 μl 2 μM α_1m, C34S-α_1m, or K(3)T-α_1m, incubated with buffer (lane 1), 2 μM cytochrome *c* (lane 2), 2 μM cytochrome *c* + 5 μM NADH (lane 3), or 5 μM NADH (lane 4). [^{14}C]IAA was added to 1 mM and the samples were separated by SDS-PAGE, stained, and analyzed by phosphoimaging.

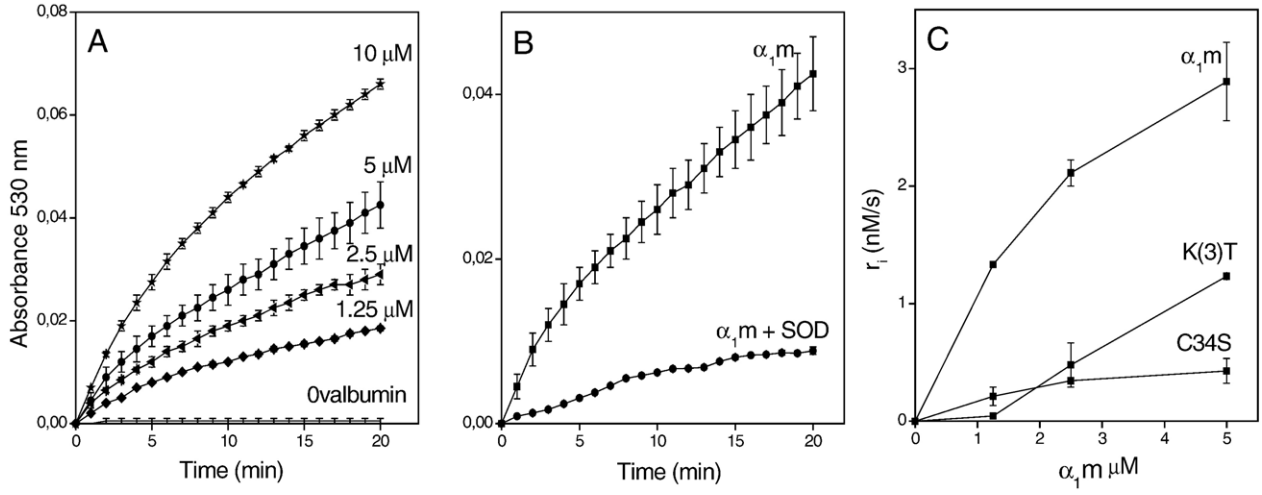

Fig. 8. Reduction of NBT by α_1m. (A) The absorbance at 530 nm of 200 μM NBT and various concentrations of α_1m, or ovalbumin at 10 μM was read at 1-min intervals. (B) The absorbance at 530 nm of 200 μM NBT and 5 μM α_1m, with or without 1.5 μM SOD, was read at 1-min intervals. (C) The initial reaction rates (r_i) were calculated from the net absorbance increase after 5 min for 200 μM NBT plus various concentrations of α_1m, C34S-α_1m, or K(3)T-α_1m and plotted as a function of the α_1m concentration. Each point shows the mean of triplicates and SE.

reductase activity, and that the reaction with cytochrome *c* is enhanced by NADH, NADPH, and ascorbate. A possible reaction scheme which explains the results and depicts α_1m as a NADH-dehydrogenase:cytochrome *c* reductase is shown in Fig. 11A. According to this model, an oxidized form of α_1m (α_1m^+) is formed by the reduction of O_2, methemoglobin, or Fe^{3+}. The superoxide anion radical, O_2^-, which is formed by reduction of O_2, subsequently reduces cytochrome *c* or NBT. The oxidized α_1m^+ is reduced again by NADH, NADPH, or ascorbate, regenerating α_1m and thereby accelerating the reduction rates.

Fig. 11B illustrates a tentative reaction mechanism for the reduction reactions. The results strongly indicate that the only free thiol group of α_1m is part of the active site for the reduction reaction. The reaction with cytochrome *c* leads to oxidation of the thiol, and blocking of the group with *N*-ethylmaleimide or changing Cys34 to Ser by site-directed mutagenesis inhibits the reaction. The three-dimensional structure of α_1m is not yet known, but modeling studies based on published lipocalin structures show that the Cys34 residue is most likely located on a solvent-exposed flexible loop lining the opening of the lipocalin pocket [31]. This is consistent with the promiscuous reaction pattern observed (α_1m can interact with many substrates and cofactors). No oxidation of the thiol group of the K(3)T-α_1m mutant was observed, implicating the Lys residues in positions 92, 118, and 130 as involved in the reaction, perhaps by creating an electronegative environment around the thiol group or by an electron transfer from the Lys residues to the Cys34 thiol (Fig. 11B). The three-dimensional model of α_1m shows that Lys 92, 118, and 130 are also located close to the rim of the lipocalin pocket and it may thus be possible for Cys 34 to interact both with the Lys groups and the electron-accepting substrates. In urine α_1m the three Lys residues carry chromophore prosthetic groups [12] and the Cys34 thiol group is partially oxidized in a nonreducable manner [32]. In

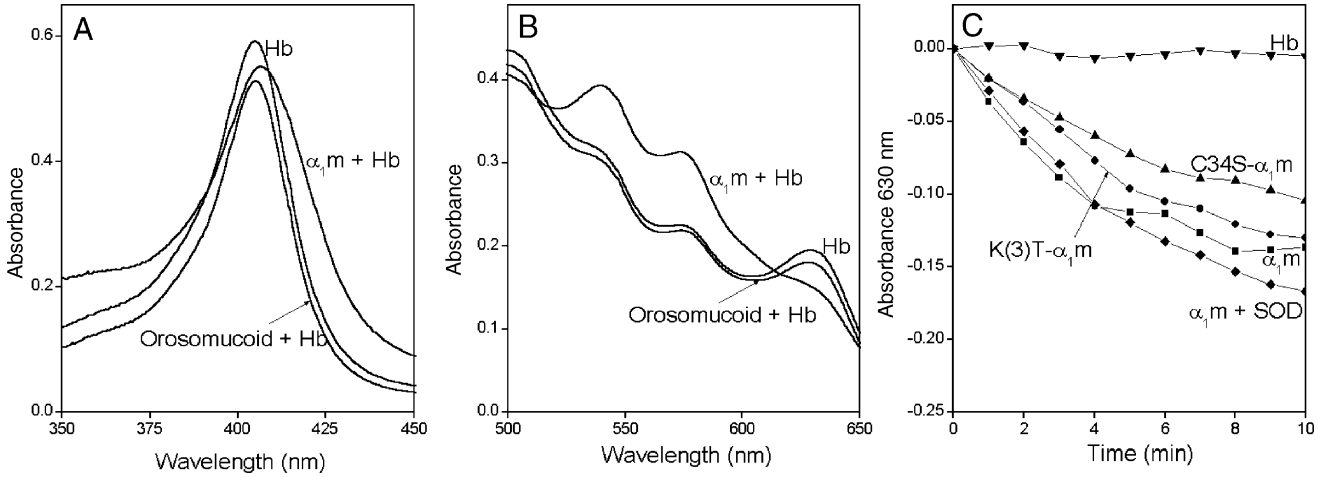

Fig. 9. Reduction of methemoglobin by α_1m. Human methemoglobin (A, 2.5 μM; B, 25 μM; C, 50 μM) was mixed with 40 μM α_1m, C34S-α_1m, K(3)-α_1m, 40 μM α_1m + 3 μM SOD, or 40 μM orosomucoid. (A and B) Absorbance spectra were read after 30 min (C) Δ-absorbance at 630 nm was read at 1-min intervals.

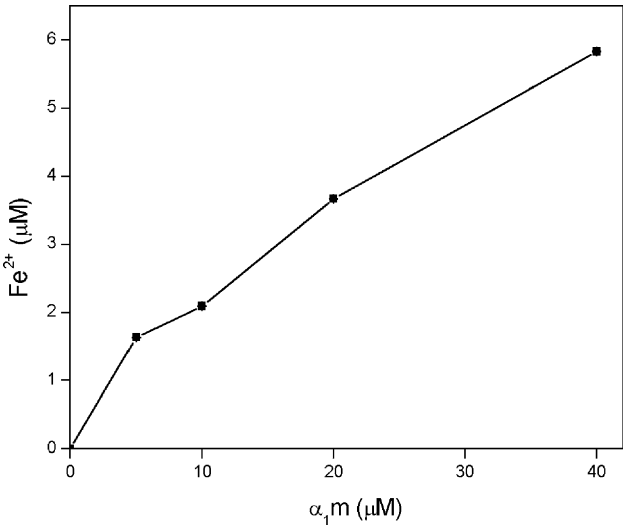

Fig. 10. Reduction of ferricyanide by α_1m. Ferricyanide ($K_3Fe^{3+}(CN)_6$), 500 μM, was incubated with various concentrations of α_1m for 90 min. The production of ferrous iron (Fe^{2+}) was determined by the phenantroline method. Each point shows the mean of triplicates and SE.

contrast, only very small amounts of chromophores are seen in recombinant α_1m. The lower reductase activity of urine and plasma α_1m may therefore be explained by irreversible blocking of these four residues.

The rate of the reduction reaction was amplified approximately 30-fold by the electron donors NADH, NADPH, and ascorbate. As illustrated in Fig. 11A, these compounds may act by regenerating α_1m, allowing a new cytochrome *c* reduction cycle to take place. This model of the catalytic mechanism is supported by several findings: (1) NADH can regenerate the reduction potential of α_1m after reaction with an excess of cytochrome *c*-Sepharose; (2) NADH accelerates the reduction reaction in a concentration-dependent manner; and (3) NADH can reduce the thiol group of α_1m. The acceleration factor by NADH was approximately the same for wild-type α_1m and the K(3)T mutant, suggesting that the Lys residues are not involved in the interaction with NADH.

It is doubtful whether NADH or NADPH can act as cofactors of α_1m in vivo. The protein is mainly found in plasma and extracellular tissue fluids [13,14,33] and is therefore codistributed with ascorbate rather than NADH and NADPH. Ascorbate also gave the highest acceleration factor for the reaction with cytochrome *c* and NBT (Table 1) and the combination of α_1m and ascorbate yielded a much stronger reaction than ascorbate's own reaction with cytochrome *c* (Fig. 5B). Interestingly, glutathione also accelerated the reduction reaction of α_1m with cytochrome *c* and NBT (not shown) and our results suggest that α_1m can interact with a wide spectrum of different biological electron donors rather than being specific for a particular cofactor.

The truncated form of α_1m, t-α_1m, showed a faster reduction rate than full-length α_1m. T-α_1m is formed by incubation with hemoglobin or erythrocyte membranes and involves processing of the C-terminal tetrapeptide LIPR [21]. This suggests that the reduction reaction of α_1m is regulated by the C-terminal tetrapeptide LIPR and that t-α_1m may be an activated form of the reductase. T-α_1m was previously shown to bind and degrade heme and an alternative explanation is that the increased reducing potential of t-α_1m is a result of degradation products of heme, for example, bilirubin, associated with the protein. T-α_1m indeed shows an absorbance spectrum consistent with binding of bilirubin [21]. Bilirubin has antioxidant properties partly due to its oxidation to biliverdin [34] and may therefore act as an electron donor to cytochrome *c* directly or using α_1m as an intermediate, explaining the increased reducing properties of t-α_1m. Addition of heme to full-length α_1m yields an α_1m-heme complex [21] which has weaker reducing properties compared to α_1m alone (not shown), arguing against α_1m-bound heme as an explanation for the effects.

There are several functional implications of the reductase activity of α_1m. (1) A biological consequence of the

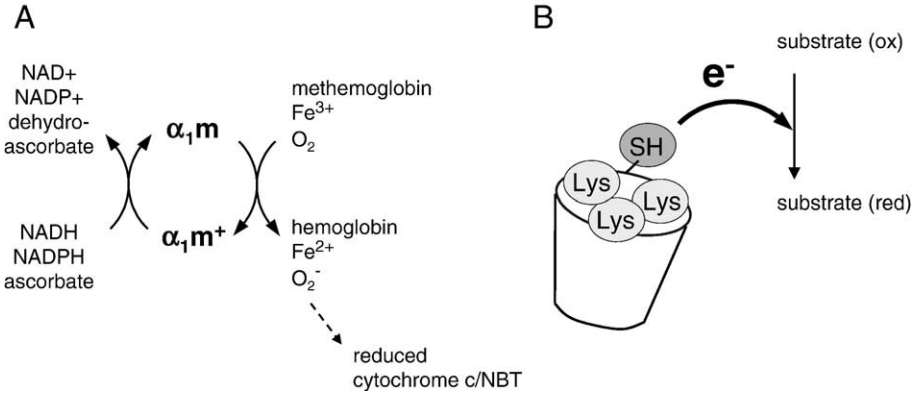

Fig. 11. Tentative reaction mechanism of α_1m. (A) α_1m reduces cytochrome *c* and NBT via formation of superoxide (the reaction is SOD inhibitable). The superoxide is hypothetically formed by reduction of molecular oxygen. α_1m also reduces methemoglobin and ferric iron directly (this reaction is not SOD inhibitable). The oxidized α_1m (α_1m^+), formed by the reduction, is reduced again by NADH, NADPH, and ascorbate. These compounds consequently accelerate the reactions. (B) The active site of α_1m is constituted by the thiol group of the unpaired cysteine in position 34, and Lys 92, 118, and 130. These four side chains are colocated at the opening of the lipocalin pocket. The thiol group, as a result of cooperation with the lysyl groups, donates an electron to the substrate and becomes oxidized.

reducing properties is antioxidation; i.e., α_1m may either reduce biological oxidants such as cytochrome *c*, methemoglobin, and ferric iron in vivo, and thereby prevent them from exerting oxidative stress on tissue components, and/or repair the oxidized target molecules by re-reducing them. (2) The reduction of ferric iron may be important for the uptake of iron in the gut or sequestering of iron by cellular ferritin. In both these cases the iron should be in its reduced form. α_1m is present in the intestinal epithelium, enriched at the tips of the microvilli [16,33], underscoring the former possibility. (3) The reducing activity of t-α_1m may be part of a heme degradation mechanism. As noted above, t-α_1m can degrade heme, possibly forming bilirubin. Heme oxygenase is an intracellular enzyme [35] that catalyzes the degradation of heme to bilirubin, CO, and free iron. The reaction, which includes several reduction steps, is assisted by NADPH:cytochrome P450 reductase and NAD(P)H:biliverdin reductase [36]. In a tentative heme degradation reaction, α_1m may be its own reductase. (4) The reductase activity could provide an explanation for the immunosuppressive properties of α_1m. Antigen-induced activation of leukocytes exploits signaling pathways which are also activated by ROS and other pro-oxidants [37,38]. The inhibition of antigen-induced proliferation and IL-2 production of lymphocytes, migration of neutrophils, IL-1-production, and oxidative burst of monocytes, which have been reported for α_1m [17–20], may therefore be an indirect result of a general reduction of pro-oxidant levels around the cells.

In conclusion, the unexpected reductase and dehydrogenase properties of α_1m described in this paper may provide a mechanistic explanation for the previously suggested functions of α_1m as a heme scavenger and immunosuppressor, and lead to the proposal of a novel function as a physiological antioxidant.

References

[1] Flower, D. R. The lipocalin protein family: structure and function. *Biochem. J.* **318:**1–14; 1996.

[2] Åkerström, B.; Flower, D.; Salier, J. P. Lipocalins: Unity in diversity. *Biochim. Biophys. Acta* **1482:**1–8; 2000.

[3] Newcomer, M.; Ong, D. Plasma retinol-binding protein: structure and function of the prototypic lipocalin. *Biochim. Biophys. Acta* **1482:**57–64; 2000.

[4] Urade, Y.; Hayaishi, O. Biochemical, structural, genetic, physiological and patophysiological features of lipocalin-type prostaglandin D-synthase. *Biochim. Biophys. Acta* **1482:**259–271; 2000.

[5] Huber, R.; Schneider, M.; Mayr, I.; Muller, R.; Deutzmann, R.; Suter, F.; Zuber, H.; Falk, H.; Kayser, H. Molecular structure of the bilin binding-protein (BBP) from *Pieris brassicae* after refinement at 2.0-Å resolution. *J. Mol. Biol.* **198:**499–513; 1987.

[6] Hieber, A. D.; Bugos, R. C.; Yamamoto, H. Y. Plant lipocalins: violaxanthin de-epoxidase and zeaxanthin epoxidase. *Biochim. Biophys. Acta* **1482:**84–91; 2000.

[7] Ekström, B.; Peterson, P. A.; Berggård, I. A urinary and plasma α_1-glycoprotein of low molecular weight: isolation and some properties. *Biochem. Biophys. Res. Commun.* **65:**1427–1433; 1975.

[8] Pervaiz, S.; Brew, K. Homology of beta-lactoglobulin, serum retinol-binding protein, and protein HC. *Science* **228:**335–337; 1985.

[9] Åkerström, B.; Lögdberg, L. An intriguing member of the lipocalin protein family: α_1-microglobulin. *Trends Biochem. Sci.* **15:**240–243; 1990.

[10] Åkerström, B.; Lögdberg, L.; Berggård, T.; Osmark, P.; Lindqvist, A. α_1-microglobulin -a yellow-brown lipocalin. *Biochim. Biophys. Acta* **1482:**172–184; 2000.

[11] Escribano, J.; Grubb, A.; Calero, M.; Méndez, E. The protein HC chromophore is linked to the cysteine residue at position 34 of the polypeptide chain by a reduction-resistant bond and causes the charge heterogeneity of protein HC. *J. Biol. Chem.* **266:**15758–15763; 1991.

[12] Berggård, T.; Cohen, A.; Persson, P.; Lindqvist, A.; Cedervall, T.; Silow, M.; Thøgersen, I. B.; Jönsson, J.Å.; Enghild, J. J.; Åkerström, B. α_1-Microglobulin chromophores are located to three lysine residues semiburied in the lipocalin pocket and associated with a novel lipophilic compound. *Protein Sci.* **8:**2611–2620; 1999.

[13] Ødum, L.; Nielsen, H. W. Human protein HC (α_1-microglobulin) and inter-alpha-trypsin inhibitor in connective tissue. *Histochem. J.* **26:**799–803; 1994.

[14] Berggård, T.; Oury, T. D.; Thørgersen, I. B.; Åkerström, B.; Enghild, J. J. α_1-Microglobulin is found both in blood and in most tissues. *J. Histochem. Cytochem.* **46:**887–893; 1998.

[15] Berggård, T.; Enghild, J. J.; Badve, S.; Salafia, C. M.; Lögdberg, L.; Åkerström, B. Histologic distribution and biochemical properties of α_1-microglobulin in human placenta. *Am. J. Reprod. Immunol.* **41:**52–60; 1999.

[16] Lögdberg, L.; Åkerström, B.; Badve, S. Tissue distribution of the lipocalin α_1-microglobulin in the developing human fetus. *J. Histochem. Cytochem.* **48:**1545–1552; 2000.

[17] Lögdberg, L.; Åkerström, B. Immunosupressive properties of α_1-microglobulin. *Scand. J. Immunol.* **13:**383–390; 1981.

[18] Méndez, E.; Fernández-Luna, J. L.; Grubb, A.; Leyva-Cobián, F. Human protein HC and its IgA complex are inhibitors of neutrophil chemotaxis. *Proc. Natl. Sci. USA* **88:**1472–1475; 1986.

[19] Wester, L.; Michaelsson, E.; Holmdahl, R.; Olofsson, T.; Åkerström, B. Receptor for alpha1-microglobulin on lymphocytes: inhibition of antigen-induced interleukin-2 production. *Scand. J. Immunol.* **48:**1–7; 1998.

[20] Santin, M.; Cannas, M. Collagen-bound α_1-microglobulin in normal and healed tissues and its effect on immunocompetent cells. *Scand. J. Immunol.* **50:**289–295; 1999.

[21] Allhorn, M.; Berggård, T.; Nordberg, J.; Olsson, M. L.; Åkerström, B. Processing of the lipocalin α_1-microglobulin by hemoglobin induces heme-binding and heme-degradation properties. *Blood* **99:**1894–1901; 2002.

[22] Allhorn, M.; Lundqvist, K.; Schmidtchen, A.; Åkerström, B. Heme-scavenging role of α_1-microglobulin in chronic ulcers. *J. Invest. Dermatol.* **121:**640–646; 2003.

[23] Berggård, T.; Thelin, N.; Falkenberg, C.; Enghild, J. J.; Åkerström, B. Prothrombin, albumin and immunoglobulin A form covalent complexes with α_1-microglobulin in human plasma. *Eur. J. Biochem.* **245:**676–683; 1997.

[24] Åkerström, B.; Bratt, T.; Enghild, J. J. Formation of the α_1-microglobulin chromophore in mammalian and insect cells: a novel post-translational mechanism? *FEBS Lett.* **362:**50–54; 1995.

[25] Wester, L.; Johansson, M. U.; Åkerström, B. Physicochemical and biochemical characterisation of human α_1-microglobulin expressed in baculovirus-infected insect cells. *Protein Expression Purif.* **11:**95–103; 1997.

[26] Babiker-Mohamed, H.; Olsson, M. L.; Winquist, O.; Nilsson, B. H. K.; Lögdberg, L.; Åkerström, B. Characterisation of monoclonal anti-α_1(microglobulin antibodies: Binding strength, binding sites, and inhibition of antigen-induced lymphocyte stimulation. *Scand. J. Immunol.* **34:**655–666; 1991.

[27] Avron, M.; Shavitt, N. A sensitive and simple method for determination of ferrocyanide. *Anal. Biochem.* **6:**549–554; 1963.

[28] Halliwell, B.; Gutteridge, J. M. C. Free radicals in biology and medicine. Oxford University Press, New York.
[29] Laemmli, U. K. Cleavage of structural proteins during the assembly of the head of bacteriophage T4. *Nature* **227:**680–685; 1970.
[30] Okado-Matsumoto, A.; Fridovich, I. Assay of superoxide dismutase: cautions relevant to use of cytochrome *c*, a sulfonated tetrazolium, and cyanide. *Anal. Biochem.* **298:**337–342; 2001.
[31] Villoutreix, B.; Åkerström, B.; Lindqvist, A. Structural model of human α_1-microglobulin: proposed scheme for the interaction with protein C. *Blood Coagul. Fibrinol.* **11:**261–275; 2000.
[32] Ekström, B.; Berggård, I. Human α_1-microglobulin. Purification procedure, chemical and physicochemical properties. *J. Biol. Chem.* **252:**8048–8057; 1977.
[33] Larsson, J.; Wingårdh, K.; Davies, J. R.; Lögdberg, L.; Strand, S. E.; Åkerström, B. Distribution of ^{125}I-labelled α_1-microglobulin in rats after intravenous injection. *J. Lab. Clin. Med.* **137:**165–175; 2001.
[34] Baranano, D. E.; Rao, M.; Ferris, C. D.; Snyder, S. H. Biliverdin reductase: a major physiologic cytoprotectant. *Proc. Natl. Acad. Sci. USA* **99:**16093–16098; 2002.
[35] Tenhunen, R.; Marver, R. S.; Schmid, J. Microsomal heme oxygenase: characterization of the enzyme. *J. Biol. Chem.* **244:**6388–6394; 1969.
[36] Ryter, S. W.; Tyrrell, R. M. The heme synthesis and degradation pathways: role in oxidant sensitivity. Heme oxygenase has both pro- and antioxidant properties. *Free Radic. Biol. Med.* **28:**289–309; 2000.
[37] Matsue, H.; Edelbaum, D.; Shalhevet, D.; Mizumoto, N.; Yang, C.; Mummert, M. E.; Oeda, J.; Masayasu, H.; Takashima, A. Generation and function of reactive oxygen species in dendritic cells during antigen presentation. *J. Immunol.* **171:**3010–3018; 2003.
[38] Reth, M. Hydrogen peroxide as second messenger in lymphocyte activation. *Nature Immunol.* **3:**1129–1134; 2002.